Effect of ATP Analogues on the Actin−Myosin Interface†

J. Van Dijk, C. Fernandez, and P. Chaussepied*

CRBM du CNRS, IFR24, 1919 route de Mende, BP 5051, 34293 Montpellier Cedex 5, France

Received January 20, 1998; Revised Manuscript Received March 20, 1998

ABSTRACT: The interaction between skeletal myosin subfragment 1 (S1) and filamentous actin was examined at various intermediate states of the actomyosin ATPase cycle by chemical cross-linking experiments. Reaction of the actin−S1 complex with 1-ethyl-3-[3-(dimethylamino)propyl]carbodiimide and *N*-hydroxysuccinimide generated products with molecular masses of 165 and 175 kDa, in which S1 loops of residues 626−647 and 567−578 were cross-linked independently to the N-terminal segment of residues 1−12 of one actin monomer, and of 265 kDa, in which the two loops were bound to the N termini of two adjacent monomers. In strong-binding complexes, i.e., without nucleotide or with ADP, S1 was sequentially cross-linked to one and then to two actin monomers. In the weak-binding complexes, two types of cross-linking pattern were observed. First, during steady-state hydrolysis of ATP or ATPγS at 20 °C, the cross-linking reaction gave rise to a small amount of unknown 200 kDa product. Second, in the presence of AMPPNP, ADP·BeF_x, ADP·AlF_4^-, or ADP·VO_4^{3-} or with S1 internally cross-linked by *N*,*N*′-*p*-phenylenedimaleimide, only the 265 kDa product was obtained. The presence of 200 mM salt inhibited cross-linking reactions in both weak- and strong-binding states, while it dissociated only weak-binding complexes. These results indicate that, in the weak-binding state populated with the ADP·P_i analogues, skeletal S1 interacts predominantly and with an apparent equal affinity with the N termini of two adjacent actin monomers, while these ionic contacts are much less significant in stabilizing the rigor actin−S1 complexes. They also suggest that the electrostatic actin−S1 interface is not influenced by the type of ADP·P_i analogue bound to the active site.

Muscle contraction and cellular movements linked to microfilaments are driven by cyclical changes in the interaction of myosin subfragment 1 (S1)[1] with actin, under the control of ATP hydrolysis (*1*). Kinetic studies on the actin−myosin ATPase reaction (*2*, *3*) and on the binding of myosin to actin (*4*) have suggested a kinetic scheme common for all myosin isoforms though with slight differences in kinetic constants (*5*). This scheme starts at the beginning of the power stroke when actin binds weakly to S1 containing ATP or the hydrolyzed ADP·P_i intermediate in its active site. The resulting transient actin−S1·ATP or actin−S1·ADP·P_i complexes are related to the collision complexes dominated by long-range electrostatic interactions (*6*, *7*). The following isomerization of S1·ADP·P_i complex and/or the release of the γP_i results in the force-generating actin−S1′·ADP·P_i or actin−S1′·ADP complex (*8*, *9*). Although this last intermediate has not been isolated yet, it should be analogous to an attached low-affinity state (A-state) of the actin−S1 interface, supposed to be constituted by both hydrophobic and ionic bonds (*4*). Finally, a second isomerization generates the actin−S1·ADP and actin−S1 complexes, populating the so-called strong or rigor conformational state (R-state), characterized by high affinities and low salt dependencies (*10*, *11*). Force would be developed during the A-state to R-state transition of the actin−S1 interface. A major goal of current researches in this field is therefore to identify the structure of the actomyosin interface for each kinetically defined state (*12*).

A detailed model of the actomyosin interface in the R-state has been built using X-ray structures of the individual proteins together with data of fiber diffraction and electron microscopy of actin filaments saturated by S1 (*13*−*15*). The model of the interface has defined four main subsites with various electrostatic and hydrophobic components. The primary and the most studied electrostatic subsite encompasses a patch of acidic residues of actin subdomain 1 (residues 1−4, 24, 25, 99, and 100) and a lysine-rich loop of S1 (residues 626−647). A great number of works using biochemical (*16*−*21*), immunological (*22*−*26*), and directed mutagenesis (*27*−*33*) approaches clearly demonstrated that this subsite is important for the actomyosin ATPase activity and that it was directly implicated in the formation of the weak-binding complexes, i.e., between actin and S1·ATP or S1·ADP·P_i intermediates. On the other hand, it was proposed to be of minor importance in stabilizing the rigor interface (*19*, *21*−*25*, *30*, *33*). The model also identified multiple hydrophobic and stereospecific contacts located in actin, mainly between subdomains 1 and 3 and within the loop of residues 40−52 of subdomain 2 of the adjacent monomer and in S1, between residues 529 and 558. Only

† This work was supported by the Centre National de la Recherche Scientifique and the Association Française contre les Myopathies.

* Corresponding author. Telephone: (33)-4-67-61-33-34. Fax: (33)-4-67-52-15-59. E-mail: Patrick@xerxes.crbm.cnrs-mop.fr.

[1] Abbreviations: AlF_4^-, aluminum fluoride; AMPPNP, 5′-adenylimido diphosphate; ATPγS, adenosine 5′-*O*-(3-thiotriphosphate); BeF_x, beryllium fluoride; DMF, dimethylformamide; EDC, 1-ethyl-3-[3-(dimethylamino)propyl]carbodiimide; NHS, *N*-hydroxysuccinimide; pPDM, *N*,*N*′-*p*-phenylenedimaleimide; S1, myosin subfragment 1; S1-(A1) and S1(A2), myosin subfragment 1 with alkali light chain A1 or A2, respectively; VO_4^{3-}, vanadate.

S0006-2960(98)00139-1 CCC: $15.00 © 1998 American Chemical Society
Published on Web 05/19/1998

few experimental studies have characterized these apolar interactions (*34*−*36*). Interestingly, a recent cross-linking study revealed that the binding of S1 residues 506−561 to actin residues 48−113, encompassing the hydrophobic subsites located on the neighbor actin subdomain 2, was influenced by the γ-phosphate moiety of the nucleotide (*37*).

Among the other probable components of the interface, one should notice a subsite, first proposed by EM reconstruction as a weak secondary binding site, between actin residues 99 and 100 and the S1 loop of residues 567−578 (*13*, *14*). This interface was not confirmed in the recent reanalysis of the EM images (*15*). However, cross-linking experiments performed under nonsaturating conditions (different from EM reconstructions) revealed that S1 could be cross-linked to residues 1−12 of two adjacent actin monomers (*38*, *39*). Since they are in close proximity on the actin surface, residues 1−12, 99, and 100 were proposed to belong to the same subsite and to interact with the positively charged loop of residues 567−578 of S1 in the substoichiometric complex. One implication of these results is that S1 interaction with the N-terminal segment of an adjacent actin, not seen either by cross-linking experiments or by EM reconstruction on the saturated actin−S1 complex, could have an important role during the formation of the physiologically relevant unsaturated rigor complex. For example, Borejdo et al. proposed that the formation of this bond could take place at the end of the power stroke and could be linked to the difference in orientation of the myosin head observed between saturated and unsaturated complexes in solution or in skeletal fibers (*40*).

The goal of the present work was to examine by chemical cross-linking experiments the significance of S1 binding to actin residues 1−12 in various transitory states of the ATPase reaction. We used cross-linking experiments mediated by EDC and NHS for three reasons. First, the cross-linking approach appears to be the most efficient way to freeze and to characterize transient protein−protein interactions as long as cross-linking occurs within a specific binding site. Second, EDC is a zero-length cross-linking reagent which has been extensively used to characterize the actin−myosin interface (*16*, *38*, *39*, *41*−*46*) and which was shown to react almost exclusively with residues 1−12 of actin (*47*). Third, the presence of NHS during the reaction promotes the formation of active ester intermediates which stabilize the activated form of the carboxyl groups (*48*). NHS increases the reaction yield, and therefore, it is essential to obtain appreciable amounts of the product containing one S1 molecule cross-linked to two actin monomers (*39*).

The actin−myosin ATPase cycle has transient states which have lifetimes that are too short to allow chemical cross-linking reaction. Therefore, we used two classes of nucleotide analogues to freeze these critical conformational states. First, we used ATP analogues, such as AMPPNP, ATPγS, and ADP·BeF_x, which induce similar global (ATP-like) changes in the three-dimensional structure of the catalytic domain of S1 (*49*) though they may exhibit slight differences regarding other structural properties in the ternary actin−S1·nucleotide complex (*50*, *51*). Second, we employed ADP·AlF_4^- and ADP·VO_4^{3-} which, again on the basis of crystallographic studies, mimic a different S1·ADP·P_i state (*52*, *53*). Moreover, we used pPDM-modified S1 which is thought to resemble structurally the S1·ADP·P_i state (*54*).

The data obtained show that one molecule of S1 can be cross-linked, i.e., interact, simultaneously with the N termini of two actin monomers in actin−S1·ADP·P_i but not in actin−S1·ATP. Moreover, the difference in salt dependencies of the cross-linking reaction and S1 binding to actin during cosedimentation experiments demonstrates that the interaction between skeletal S1 and the N-terminal residues of two monomers is predominant in the weak- but much less important in the strong-binding states.

MATERIALS AND METHODS

Materials. 1-Ethyl-3-[3-(dimethylamino)propyl]carbodiimide (EDC), *N*-hydroxysuccinimide (NHS), and ADP were purchased from Sigma. α-Chymotrypsin and sodium vanadate were obtained from Worthington biochemicals and Aldrich, respectively. NaF, $BeSO_4$, and $AlCl_3$ were from Merck. ATP, AMPPNP, and ATPγS were obtained from Boehringer Mannheim. NAP10 columns were supplied by Pharmacia.

Protein Preparations. Rabbit skeletal myosin was prepared as described by Offer et al. (*55*). S1 was obtained by chymotryptic digestion of myosin filaments (*56*). S1(A1) and S1(A2) isoforms were separated by ion exchange chromatography as described previously (*57*). The two S1 isoforms were used either separately or combined without producing substantial change in the cross-linking data. Rabbit skeletal F-actin was prepared from acetone powder and further purified by two cycles of polymerization−depolymerization (*58*). Protein concentrations were determined spectrophotometrically using extinction coefficients $A^{1\%}_{280nm}$ of 5.7 cm^{-1} for myosin, 7.5 cm^{-1} for S1, and 11.0 cm^{-1} for actin. The molecular masses used were 500, 115, and 42 kDa for myosin, S1, and actin, respectively.

pPDM Modification of S1. S1 at 60 μM in 100 mM HEPES and 2.5 mM $MgCl_2$ (pH 8.0) was incubated for 50 min at 4 °C in the presence of 2.5 mM ADP and a 1.5-fold molar excess of pPDM (10 mM stock solution in DMF; *59*). The cross-linking reaction was stopped by 50 mM 2-mercaptoethanol. To remove un-cross-linked S1, the sample was centrifuged for 15 min at 380000*g* in the presence of 30 μM F-actin and 50 mM NaCl (*60*). The supernatant containing pPDM S1 was finally purified on a NAP10 column equilibrated with cross-linking buffer [30 mM MOPS and 2.5 mM $MgCl_2$ (pH 7.0)].

Cosedimentation Experiments. F-actin (45 μM) and S1 derivatives (15 μM) were mixed in cross-linking buffer [30 mM MOPS and 2.5 mM $MgCl_2$ (pH 7.0)], supplemented with 15 mM NHS, with or without 200 mM NaCl. To obtain complexes in the strong-binding states, the actin−S1 mixture was preincubated for 5 min at 20 °C in the absence or in the presence of 2 mM ADP. Complexes in the weak-binding states were prepared under two different experimental conditions. First, with nucleotide analogues trapped in the active site, S1 was preincubated with the analogues for 15 min at 20 °C and then mixed with actin. Nucleotide analogues were 2 mM ADP in the presence of 10 mM NaF and 2 mM $BeSO_4$ for forming S1·ADP·BeF_x, 10 mM NaF and 2 mM $AlCl_3$ for forming S1·ADP·AlF_4^-, and 2 mM VO_4^{3-} (stock solution prepared according to ref *61*) for forming S1·ADP·VO_4^{3-} complexes. Second, with nucleotide analogues which were not trapped, 20 mM Mg·ATP,

Mg·ATPγS, or Mg·AMPPNP was added to the actin−S1 mixture just prior to centrifugation. The change in ionic strength induced by the analogues was corrected by adding the desired amount of NaCl. All the samples were centrifuged at 380000*g* for 15 min at 20 °C. The supernatant (containing free S1 and traces of monomeric actin) and the pellet (containing the actin−S1 complexes) were analyzed by SDS−PAGE, and the amount of protein was estimated by densitometric analysis. The amount of free S1 in the supernatant was also estimated by Bradford's method (*62*).

Cross-Linking Experiments. Actin−S1·nucleotide complexes were prepared as described for the cosedimentation experiments. ATP, ATPγS, and AMPPNP concentrations were changed where indicated. Cross-linking reactions were initiated by the addition of 15 mM EDC (freshly dissolved in cross-linking buffer), and they were stopped at the times indicated by incubating an aliquot of the mixture in 2 volumes of boiling Laemmli solution for 5 min [50 mM HEPES, 2% (w/v) SDS, 1% 2-mercaptoethanol, and 50% (v/v) glycerol]. The cross-linked products were analyzed by SDS−PAGE.

Light Scattering Measurements. Light scattering measurements were carried out on a Kontron SFM 25 spectrofluorimeter. Light scattering intensity was monitored at 90° with respect to the incident light at a wavelength of 400 nm at 20 °C.

SDS−PAGE. Gel electrophoresis was performed as described by Laemmli (*63*) using a 4 to 18% gradient polyacrylamide gel. Un-cross-linked and cross-linked proteins were stained with Coomassie blue. Densitometric analysis of the gels was carried out with a Shimadzu CS 930 high-resolution gel scanner equipped with a computerized integrator.

RESULTS

Cosedimentation of the Actin−S1 Complex with or without Nucleotide Analogues. The presence and the type of nucleotide bound to the active site of S1 dramatically influence the equilibrium between the weak (with actin−S1·ATP and actin−S1·ADP·P_i)- and the strong (with actin−S1·ADP and actin−S1)-binding states. To set up the optimum experimental conditions for cross-linking experiments, we first estimated the amount of actin−S1 complex formed in the presence of each nucleotide analogue, by cosedimentation experiments (Figure 1). The data highlighted two classes of complexes. The first class was obtained in the absence of nucleotide or in the presence of ADP, with more than 95% of the complex sedimented at low ionic strength. This class presented a low salt dependence since 200 mM NaCl diminished only to 96 and to 64% the amount of S1 bound to actin in the absence and in the presence of ADP, respectively. The second class was formed with all the so-called ATP and ADP·P_i analogues such as ATP, AMPPNP, ATPγS, ADP·BeF_x, ADP·AlF_4^-, ADP·VO_4^{3-}, and pPDM−S1. It was characterized by less than 20% (except for pPDM−S1 with 27.8%) of the actin−S1 complex in the pellet, at low ionic strength. Although pPDM−S1 had an apparently higher affinity for actin at low ionic strength, it was comparable to all the analogues of this class in 200 mM NaCl with less than 3% of pelleted materials.

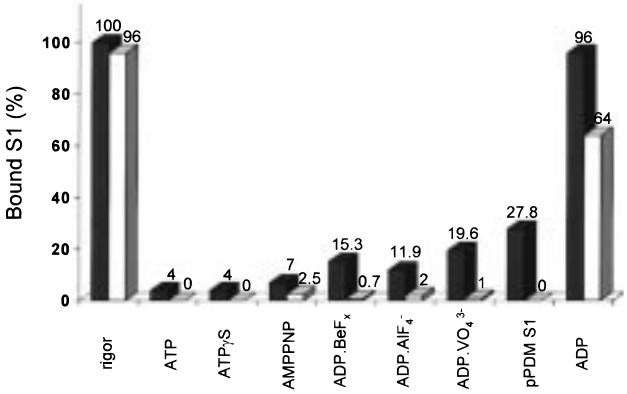

FIGURE 1: Cosedimentation of the actin−S1 complex in the presence of various nucleotide analogues. Actin−S1·nucleotide complexes were prepared by mixing actin (45 μM) and S1 (15 μM) alone or combined with various nucleotide analogues in 30 mM MOPS and 2.5 mM $MgCl_2$ (pH 7.0) as described in Materials and Methods. Protein mixtures were centrifuged for 15 min at 380000*g*, in the absence (filled bars) or in the presence (empty bars) of 200 mM NaCl, as described. The amounts of actin−S1 complex in the pellet and of free S1 in the supernatant were estimated by densitometry of SDS−PAGE and by the Bradford method for S1 in the supernatant. Values are means of two independent experiments.

These results confirmed two states of the actin−S1 interface, depending on the nucleotide present in the S1 active site: the strongly bound state (with ADP or no nucleotides) and the weakly bound state (with γP_i containing nucleotides or their analogues).

Cross-Linking of the Actin−S1 Complex in the Rigor State. Cross-linking reaction mediated by EDC and NHS between actin and S1 or the entire molecule of myosin has been well documented in the absence of nucleotide, i.e., for the complex in the rigor state (*38*, *39*). The gel electrophoresis pattern of the reaction performed at an actin/S1 ratio of >1 always revealed four cross-linking products with apparent molecular masses of 165, 175, 200, and 265kDa as depicted in Figure 2A. The 165 and 175 kDa products were found to contain one S1 molecule bound to N-terminal residues 1−12 of one actin monomer (*43*), while the 265 kDa band resulted from the linkage of one S1 simultaneously to the same N-terminal segment of two adjacent actin monomers (*38*, *39*). In the 165 kDa band, the cross-linking site is in the lysine-rich loop of residues 626−647 of S1; in the 175 kDa product, the site has been proposed in the S1 loop of residues 567−578 (*42*). These S1 segments are also implicated in the formation of the covalent $actin_2$−S1 product of 265 kDa (*64*). The cross-linking sites implicated in the less abundant 200 kDa product are not known, although this product is composed of one S1 bound to one actin molecule (*65*). A schematic representation of these different cross-linking sites is illustrated in Figure 3. Cross-linking reaction depends on the experimental conditions (proteins, EDC and NHS concentrations, pH, temperature, etc.), but the time course of the formation of the cross-linking products was always unchanged under rigor conditions; the 165, 175, and the 200 kDa products were generated first, followed by the doubly cross-linked 265 kDa adduct (Figure 2A; *39*). As shown in Figure 2B, the nature of the products and the time course of the reaction were not affected by the presence of 2 mM ADP which is sufficient for formation of the ternary actin−S1·ADP complex. Only the yield of the reaction was lower in the presence of ADP, probably due to a slightly lower amount

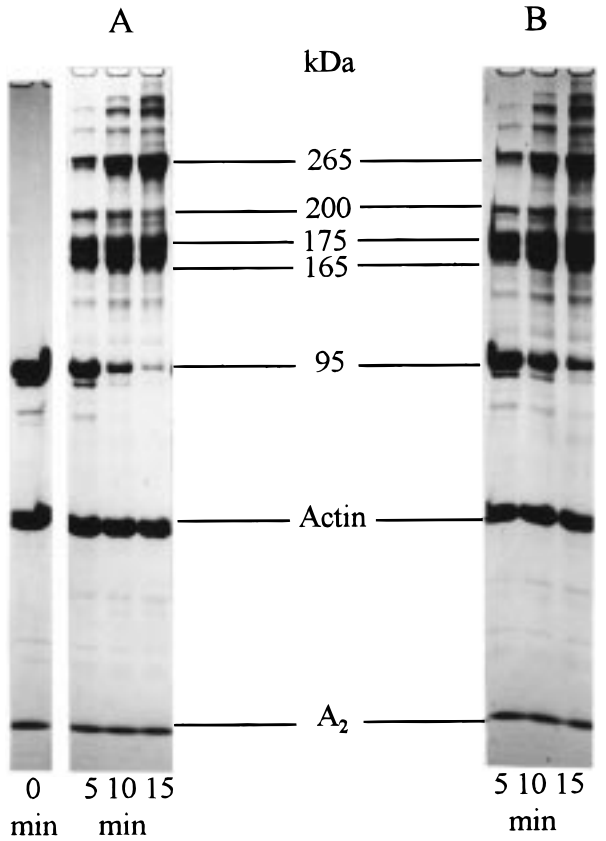

FIGURE 2: EDC-induced cross-linking of the actin−S1 complex in the rigor states. Cross-linking reactions were performed on a mixture of 45 μM actin and 15 μM S1 as described in Materials and Methods in the absence (A) or presence (B) of 2 mM Mg·ADP. Aliquots were withdrawn after reaction for 0, 5, 10, and 15 min and run on SDS−PAGE. The 95 kDa band is S1 heavy chain, and the 165, 175, 200, and 265 kDa are cross-linking products as described in detail in the text.

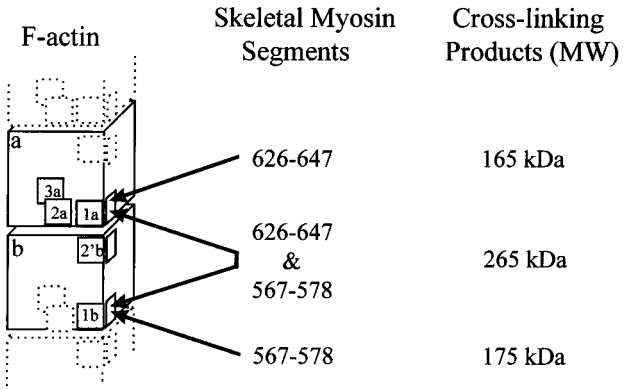

FIGURE 3: Schematic drawing of the EDC- and NHS-induced cross-linking sites and covalent products obtained with the strong actin−S1 complexes. Two actin monomers (a and b) are represented. Cross-linking products of 165, 175, and 265 kDa correspond to covalent linkages between residues 1−7 of actin with S1 loops of residues 626−647, 567−578, and both 626−647 and 567−578, respectively. S1 binding subsites on actin are as reported in refs *13*−*15*: subsite 1 (residues 1−4, 24, 25, 99, and 100), subsite 2a (residues 144−148 and 339−354), subsite 2′b (residues 40−42), and subsite 3 (residues 322−333).

of complex formed (Figure 1). Note that under rigor conditions, the presence of NHS allowed the reaction to produce a nearly 100% yield which was hardly obtainable in its absence (*41*). Therefore, NHS reaction with carboxylate groups did not significantly affect their proximity to S1

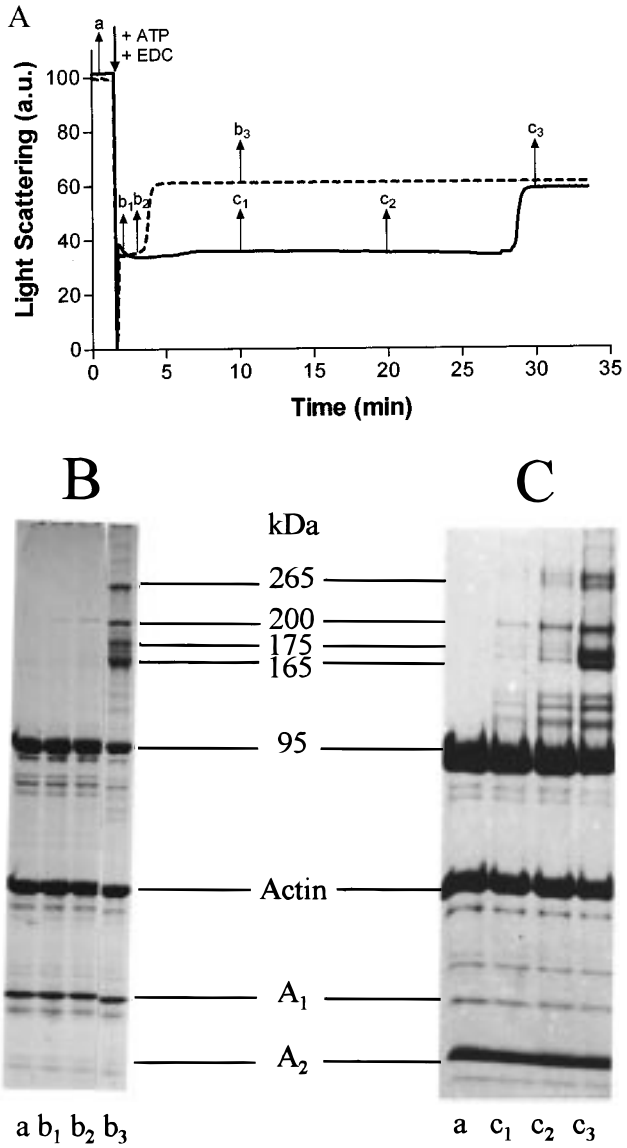

FIGURE 4: Time course of actin−S1 cross-linking during ATP hydrolysis. The ATPase and cross-linking reactions of the actin−S1 complex were monitored by light scattering at 400 nm (A) and by SDS−PAGE (B and C), respectively. Actin (45 μM) and S1 (15 μM) were mixed at 20 °C in cross-linking buffer [30 mM MOPS, 2.5 mM $MgCl_2$, and 15 mM NHS (pH 7.0)], and 4 mM (A, dashed line; B) or 20 mM (A, solid line; C) Mg·ATP and 15 mM EDC were successively added to the protein mixture with a 10−15 s interval as indicated. Aliquots of the reaction mixture were withdrawn at the times indicated by arrows (labels a, b_1−b_3, and c_1−c_3) and analyzed by gel electrophoresis as described in Materials and Methods.

side chains. This is probably due to the fact that the cross-linking sites contain several carboxyls which are unlikely to be simultaneously modified by EDC and NHS (*47*).

Cross-Linking of the Actin−S1 Complex during ATP Hydrolysis. Cross-linking experiments with the actin−S1 complex during steady-state ATPase reaction utilized two complementary approaches, light scattering measurements and gel electrophoresis. Using light scattering experiments, we could estimate the time spent in the weak actin−S1 binding state which results in a dramatic decrease in the light scattering value over the course of the ATPase reaction (Figure 4A). At the end of the reaction, the strong actin−S1·ADP binding state was then characterized by a higher,

though intermediate, light scattering value. Note that the presence of EDC and NHS did not affect, at least qualitatively, the behavior of the light scattering trace (*66*) and that the use of two different ATP concentrations only changed the time spent by the complex in the weak-binding state (Figure 4A). Gel electrophoresis analysis of the protein mixtures during ATPase reactions showed different cross-linking patterns in weak- and strong-binding states. In the former, the 200 kDa product was almost exclusively produced (Figure 4B, lines b_1 and b_2; Figure 4C, lines c_1 and c_2), while in the latter, the four bands of 165, 175, 200, and 265 kDa were generated (panels B and C of Figure 4, lines b_3 and c_3). Note that the overall patterns of the cross-linking products in the weak- and strong-binding states were identical for 4 and 20 mM ATP, though the rapid hydrolysis of 4 mM ATP authorized only a low cross-linking yield during the steady-state ATPase reaction (with a very faint 200 kDa band; Figure 4B, lines b_1 and b_2). The difference in the time course of the cross-linking reaction observed between 4 and 20 mM ATP, however, clearly established the specificity of the cross-linking patterns which were only due to the binding state of the actin−S1 interface during ATPase reaction.

The cross-linking reaction during ATP hydrolysis was also carried out in the presence of ATPγS. This analogue has the advantage of being slowly hydrolyzed by myosin and myosin derivatives due to a slow cleavage step, and most important, the hydrolysis is not activated by actin binding (*67*, *68*). As with ATP, cross-linking experiments were performed at two ATPγS concentrations, 4 and 20 mM. As depicted in Figure 5A,B, the patterns of cross-linking reactions were very comparable to those obtained with ATP. At 4 mM ATPγS, the 200 kDa band was first generated during the hydrolysis time course. When all the ATPγS was consumed (after reaction for 15 min as judged by the change in the light scattering traces; data not shown), the four cross-linking products were obtained. At 20 mM ATPγS, the 200 kDa band was observed during the all cross-linking reaction since at 15 min, hydrolysis of ATPγS was not complete yet (Figure 5B). Note that a small amount of the 265 kDa band was also generated at 20 mM ATPγS.

Cross-Linking of Actin-S1 in the Presence of Various ATP Analogues. We first used AMPPNP which is not hydrolyzed by S1 or acto-S1 and which was recently proposed to interact with S1 in a manner similar to that of ATPγS (*49*). Cross-linking experiments in the presence of AMPPNP and ATPγS, however, generated quite different cross-linking patterns. In the presence of 4 mM AMPPNP, the four cross-linking products were observed in a time course slightly similar to that seen under rigor conditions (not shown), while with 20 mM AMPPNP, the 265 kDa product was virtually the only product detected by SDS−PAGE (Figure 6D). The difference between 4 and 20 mM could easily be accounted for by a low dissociating effect of AMPPNP on the actin−S1 complex since cosedimentation assays revealed that 35 and 7% of the complex were formed in the presence of 4 and 20 mM AMPPNP, respectively (experiments performed under identical final ionic strength conditions; data not shown). Interestingly, even under identical conditions which facilitated the formation of weak ternary actin−S1·nucleotide complexes, the cross-linking patterns were totally different from those obtained with the ternary actin−S1·ATPγS complex (Figure 5B).

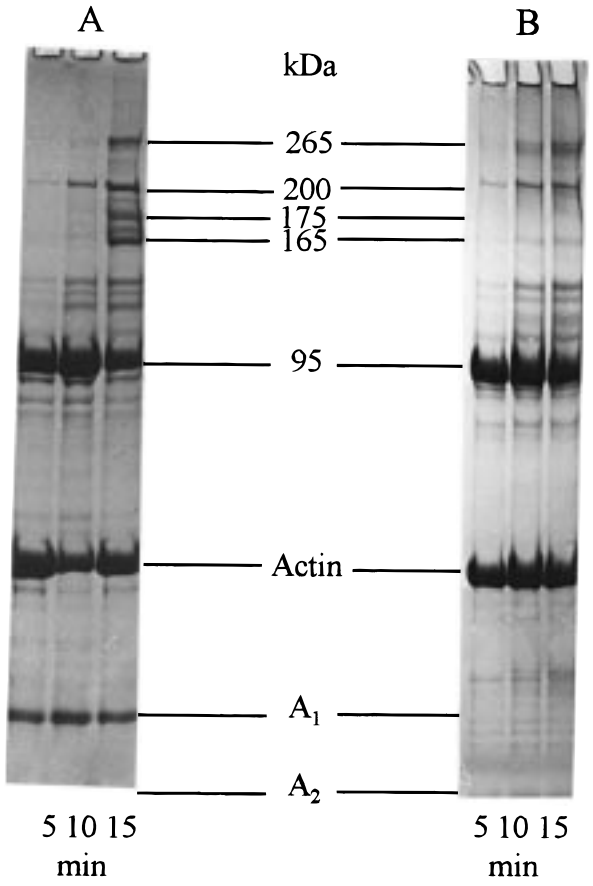

FIGURE 5: EDC-induced cross-linking of the actin−S1 complex in the presence of ATPγS. Cross-linking experiments were performed as described in Materials and Methods in the presence of 4 mM (A) or 20 mM (B) Mg·ATPγS. Aliquots were withdrawn after reaction for 5, 10, and 15 min and were run on SDS−PAGE.

To overcome the low affinity of AMPPNP for the actin−S1 complex, we also used ATP analogues that could be trapped in the S1 active site, giving rise to stable and long-life S1·nucleotide complexes. Figure 6 (panels A−C) describes cross-linking experiments performed in the presence of ADP·BeF_x, ADP·AlF_4^-, and ADP·VO_4^{3-}. In all cases, the 265 kDa product was almost exclusively formed, even during the earliest time of the reaction. Therefore, S1 cross-linked, and probably interacted, simultaneously the N-terminal segments of two adjacent actin monomers in these weak actin−S1·nucleotide complexes.

Effects of Salts on the Cross-Linking Reaction in the Strongly and Weakly Bound States. To study the salt sensitivity of the cross-linking products obtained in the strong- and weak-binding states, we compared the effect of 200 mM NaCl on the cross-linking pattern obtained with native S1 and with pPDM−S1. We used pPDM−S1 as a weak-binding state analogue mainly because its structure has the ability to mimic the S1·ATP or S1·ADP·P_i state in the absence of added nucleotide. The cross-linking pattern obtained with the actin−pPDM−S1 complex was indeed very similar to that obtained in the presence of trapped nucleotides or high AMPPNP concentrations with a predominant 265 kDa product (Figure 7C), and consequently, it was quite different from that of the rigor complex (Figure 7A). In both the rigor and weak-binding complexes, however, salt had a dramatic effect on the cross-linking reaction with almost a total loss and about 60% reduction

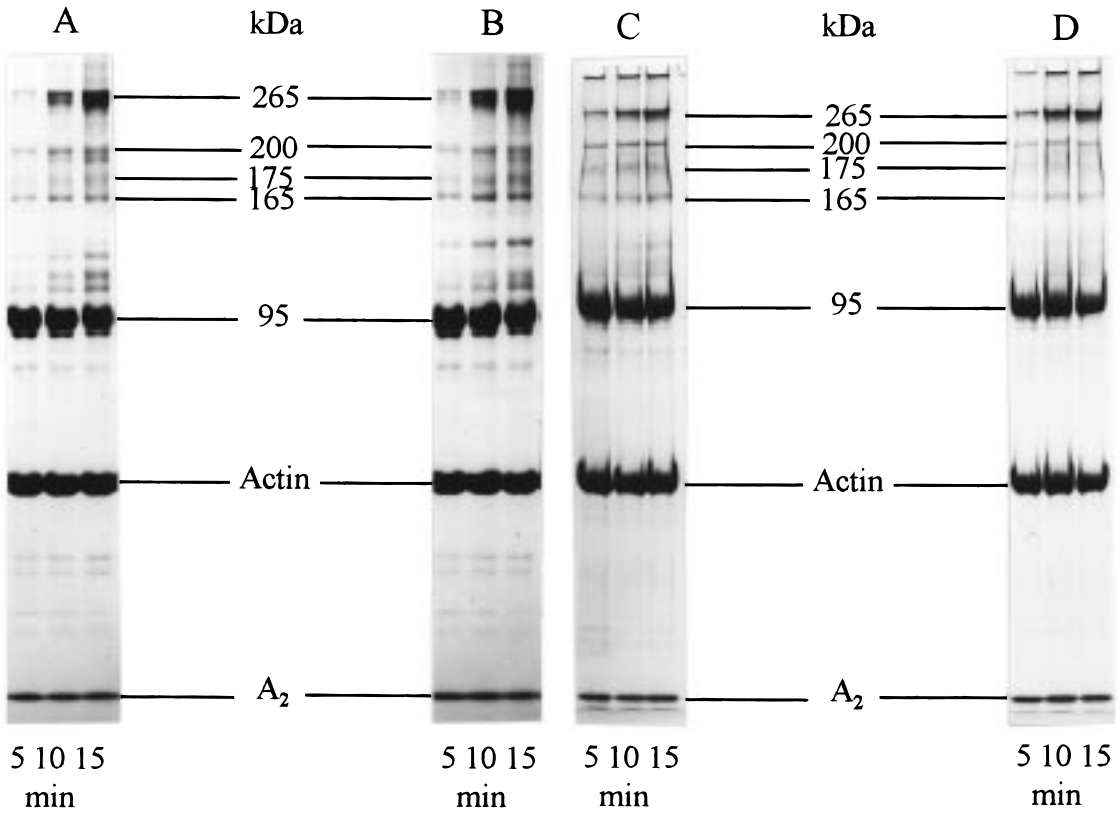

FIGURE 6: Effect of ADP·P_i analogues on actin−S1 cross-linking. Cross-linking reactions were performed with 45 μM actin and 15 μM S1 as described in Materials and Methods in the presence of 2 mM Mg·ADP·BeF_x (A), Mg·ADP·AlF_4^- (B), Mg·ADP·VO_4^{3-} (C), and 20 mM Mg·AMPPNP (D). Aliquots were withdrawn after 5, 10, and 15 min and analyzed on a polyacrylamide gel.

of EDC reaction on actin−pPDM−S1 (Figure 7D) and actin−S1 complexes, respectively (Figure 7B). It is interesting to note that, while the cross-linking at the N-terminal part of actin was dependent on salt, the amount of complex formed in the strong-binding states was not (Figure 1). On the other hand, the loss of cross-links in weak complexes was expected since very little complex could be formed under such high salt concentrations (Figure 1).

DISCUSSION

Our results demonstrate that the interaction of S1 with the N-terminal segment of actin varies dramatically during the actin−S1 ATPase cycle. More particularly, time courses of EDC- and NHS-induced cross-linking reaction reveal at least three states of the actin−S1 interface, depending on the nucleotide present in the S1 active site, as illustrated in Figure 8.

Cross-Linking in the Strong-Binding States. EDC- and NHS-induced cross-linking reactions performed on rigor actin−S1 complexes can be described as two-step cross-linking processes. First appear the covalent products containing S1 bound to the N-terminal segment of either of the two actin monomers involved in S1 interaction. Second, the accumulation of actin−S1 covalent products leads to the slow formation of the $actin_2$−S1 derivatives. The slowness of the double cross-linking reaction can be due to three reasons: (i) nonspecific binding during the second cross-linking reaction, (ii) chemical reaction is rather slow and does not allow rapid formation of covalent linkages, and (iii) S1 interaction with these two actin subsites is unstable so real contacts are rare. The first reason can be ruled out since the doubly cross-linked product is fully active (*69*; J. Van Dijk et al., manuscript in preparation). On the other hand, both of the two last reasons are possible, but we favor the second one because, when actin is activated first and then mixed with S1, we obtain identical cross-linking time courses (result not shown) and because there is evidence indicating that the N-terminal part of actin is accessible in the rigor complexes (*21*−*25*).

The pattern of the cross-linking time course is quite unchanged in the presence of ADP, in good agreement with the absence of profound modification at the interface upon ADP binding (*70*). On the other hand, it has been shown that ADP reduces the net electric charge of the actin−S1 interface (*10*). Our data suggest that this decrease of the ionic interaction does not take place at the S1 subsite located on the actin segment of residues 1−4.

Cross-Linking in the Weak Actin−S1·ATP State. The effect of nucleotides on the actin−S1 interface was previously studied by EDC-induced cross-linking experiments (*16*, *44*−*46*). For example, it was discovered that within the same subsite (between the actin N-terminal segment of residues 1−4 and the S1 loop of residues 626−647) the presence of nucleotide induces a shift in the cross-linked residues (*16*). Nevertheless, in these studies, NHS was not used, and therefore, they did not have access to the entire set of cross-linking products such as the 200 and 265 kDa entities. As reported in this work, the ability of revealing these two products is of particular importance since they are specifically regulated by nucleotide analogues.

ATP has the advantage of being the natural substrate for the actin−myosin system, but it has the handicap of

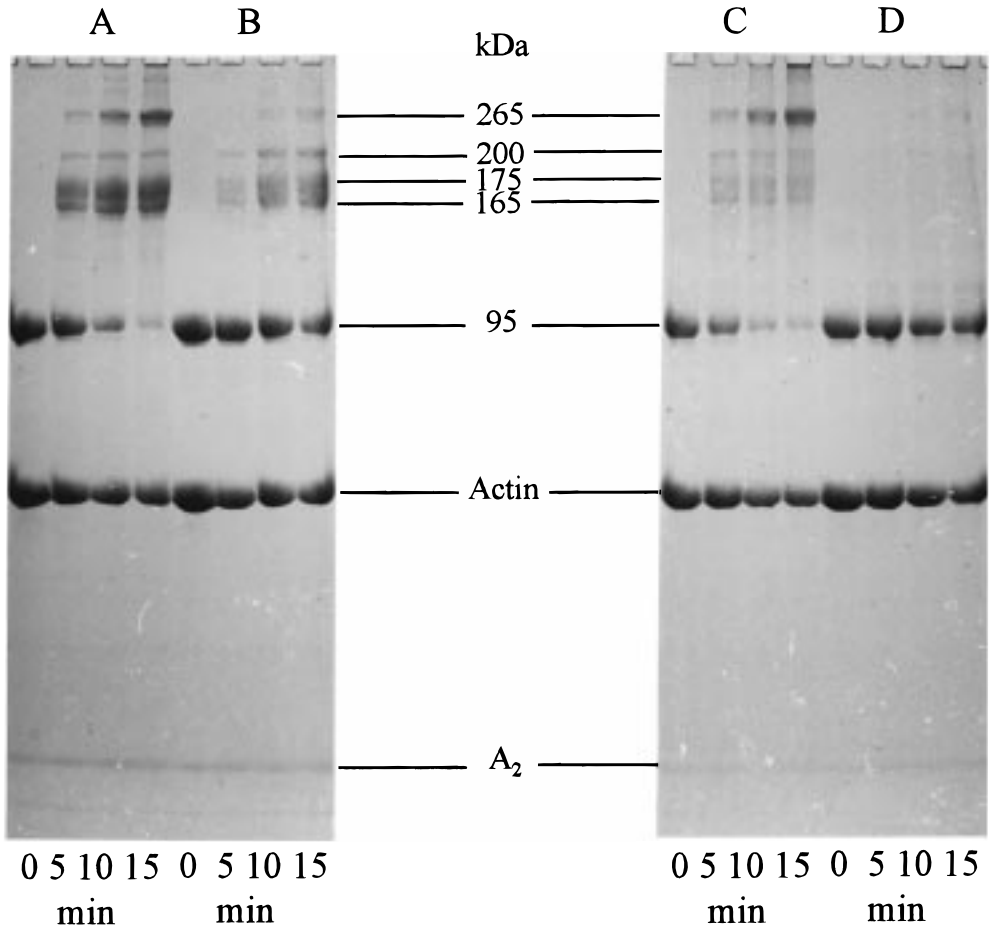

FIGURE 7: Effects of salt on the cross-linking reaction of actin−S1 complexes in the strong- and weak-binding states. Cross-linking reactions were performed between actin and native S1 (A and B) or pPDM-treated S1 (C and D) in the absence (A and C) or in the presence (B and D) of 200 mM NaCl as described in Materials and Methods.

populating, though with different yield, all the intermediate states of the ATPase reaction. Under our experimental conditions, the limiting step of the reaction appears to be the cleavage step of the $\beta-\gamma$ phosphate bond so that the most populated state is the actin−S1·ATP intermediate (*71*−*73*). We found that, in the presence of ATP, only a faint unidentified covalent product of 200 kDa is generated. Interestingly, the data obtained with ATP are identical to those obtained with ATPγS which was also proposed to populate predominantly the actin−S1·ATP state (*49*, *67*, *68*). One should note, however, that a 265 kDa band of very minor importance was also present with a high concentration of ATPγS. Since the 265 kDa product is favored in the actin−S1·ADP·P_i complexes (discussed below), this result may indicate that the limiting step of ATPγS hydrolysis is slightly shifted to the product release step under these experimental conditions. In a general point of view, it is interesting that the close resemblance between the structure and activity of S1·ATP and S1·ATPγS was also described in small G-proteins interacting with GTP and GTPγS (*74*).

Attempts to identify the cross-linking sites in the actin−S1·ATP state were unsuccessful due to the low amount of the 200 kDa adduct. Previous studies proposed that a similar 200 kDa product obtained with a more hydrophobic reagent [*N*-(ethoxycarbonyl)-2-ethoxy-1,2-dihydroquinoline] was generated by S1 cross-linking to the actin segment of residues 40−113 (*7*). However, a direct extrapolation of this result to the EDC- and NHS-induced 200 kDa product is not straightforward. On the other hand, the low intensity of this band can be associated with a weak interaction which may stress some question regarding its specificity. A lack of specificity, in this case, would not be due to the high nucleotide concentration (20 mM) employed since an identical result is also observed at 4 mM nucleotide and since the same high concentration of AMPPNP induces a quite different cross-linking pattern. However, one should keep in mind that the actin−S1·ATP intermediate, stabilized in the 200 kDa product, could represent a collision complex formed in the early time of the ATPase cycle and that such collision complexes lead sometimes to nonproductive interactions (*76*).

Cross-Linking in the Weak Actin−S1·ADP·P_i State. The results obtained with S1·AMPPNP, S1·ADP·BeF_x, S1·ADP·AlF_4^-, S1·ADP·VO_4^{3-}, and pPDM−S1 show, for the first time, that these S1 intermediates interact simultaneously with the N-terminal segments of two actin monomers. The dramatic difference in the cross-linking time courses obtained with S1 or S1·ADP and with these intermediates clearly demonstrates the relative importance of these binding subsites in stabilizing the strong and weak actin−S1·ADP·P_i complexes. In strong-binding complexes, the time scale needed to reach the covalent $actin_2$−S1 adduct and the high salt sensitivity of the cross-linking reaction are in contrast with the millisecond time scale necessary for S1 to interact with actin and with the low salt dependence of the reversible rigor complex. These discrepancies confirm

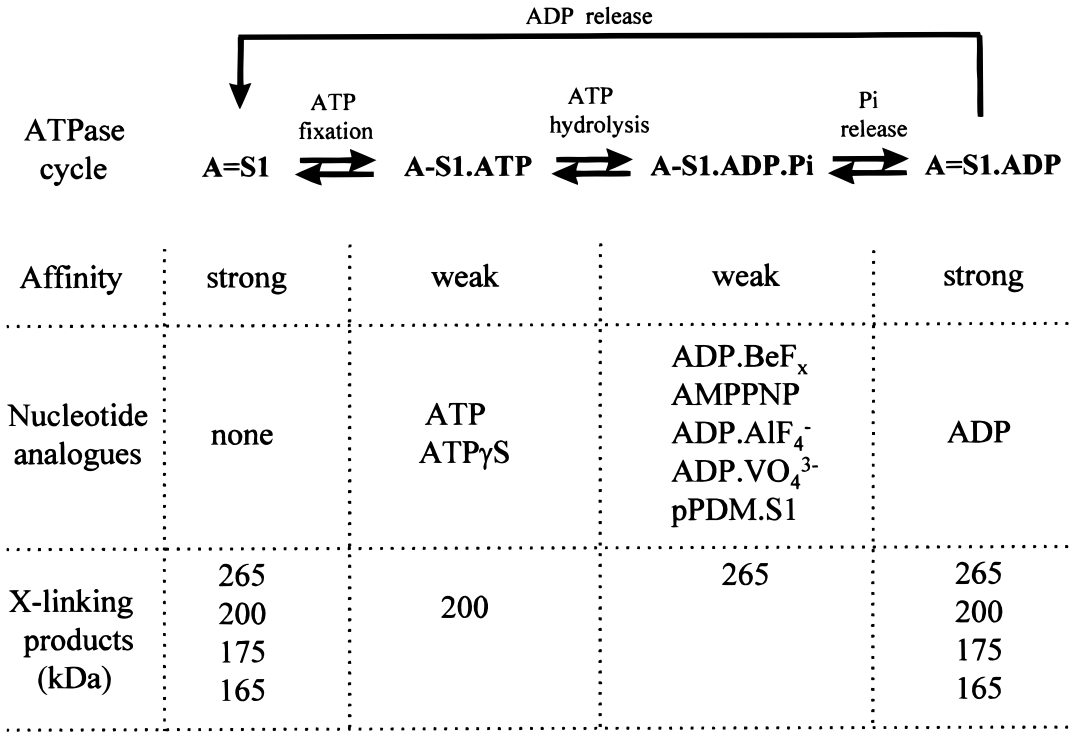

FIGURE 8: Schematic illustration of the relationship between the actin−S1 ATPase cycle and the cross-linking products obtained with each nucleotide analogue. Analogues are classified with regard to the cross-linking pattern they promote. The strength of the actin−S1 interaction is also indicated. See the text for more details.

the nonessential character of these ionic components in the stabilization of the strong-binding interface (*19*, *21*−*25*, *30*, *33*). In weak-binding complexes, on the other hand, the simultaneous cross-linking of S1 to two actin monomers early in the reaction time course together with a comparable salt effect on the cross-linking reaction and on the interaction show that these two subsites are important components of the weak-binding interface. This conclusion does not contradict the fact that the S1·nucleotide complex may interact with subdomain 2 of the second actin monomer (*37*), and it is supported by the fact that an antibody directed against the S1 loop of residues 567−574 has a strong inhibitory effect on the movement of actin filaments in in vitro motility assays (*77*).

The slight differences in the amount of S1 bound to actin observed in cosedimentation experiments in the presence of ATP analogues are probably due to differences in the binding constants of these analogues for S1 bound to actin, i.e., the tendency to form the ternary actin−S1·nucleotide complexes (*78*, *79*). This could imply that parts of these complexes, which are not in ternary form, are in the rigor state. Nevertheless, cross-linking patterns obtained under identical conditions are very similar for all the ADP·P_i analogues tested as was observed for cross-linking of the apolar actin−S1 subsites (*37*). This suggests that most, if not all, of the sedimented actin−S1 complex is in the weak-binding state.

Another matter with these ATP analogues is their direct effect on the structure of actin filament. Such a possibility is rather unlikely since binding of ADP·VO_4^{3-}, ADP·BeF_x, or ADP·AlF_3^- to actin filament does not change significantly actin−S1 ATPase activity or the sliding velocity of actin filaments in in vitro motility assays (*80*, *81*).

A drawback with chemically modified S1 derivatives such as pPDM−S1 is the possible nonspecific structure induced by the protein modification. For example, some nonelectrostatic interactions were found to remain in pPDM−S1 (*82*). However, the data confirm that pPDM−S1 is a good S1·ADP·P_i analogue. Moreover, the identity in the results obtained with pPDM−S1 and the four other S1·ADP·P_i analogues reveals that the exclusive formation of the 265 kDa product does not come from nonspecifically bound nucleotide since in the case of pPDM−S1 there is no free nucleotide.

Relation with Other Structural Data. A global analysis of our data reveals that all the cross-linked product obtained in the presence of the nucleotide analogues are also formed in the rigor actin−S1 complex. Only the intensity and the time course of the reaction differ. This observation strengthens the choice of the cross-linking approach since it rules out nonspecific cross-linking reactions always possible in the weakly bound state of the actin−S1·nucleotide complexes.

On the basis of the high-resolution X-ray structure of the catalytic domain of *Dictyostelium* S1 in complex with various analogues, it was proposed that ADP·BeF_x, ATPγS, and AMPPNP mimic ATP whereas ADP·AlF_4^- and ADP·VO_4^{3-} resemble the ADP·P_i transition states (*49*, *52*, *53*). An important conclusion of this work is that these two sets of structure are not related to two different classes of actin−S1 interfaces. This implies that the changes in S1 structure linked to the lever arm hypothesis may not be directly associated with changes in the actin−S1 interface. Conversely, S1·ATPγS which exhibits apparently a structural identity with S1·AMPPNP or S1·ADP·BeF_x (with differences smaller than 1 Å; *49*) cross-links to actin in a very divergent manner. These data are not totally inconsistent since the two S1 loops involved in the chemical cross-link which are not visible in the crystal structures may have different

accessibility depending on the nucleotide bound to the active site. On the other hand, molecular dynamic calculations suggested that these two loops would be inaccessible in the presence of ATP (*83*). Our experimental results show that this is obviously not the case. Finally, it remains unexplained how the structure of S1·ADP and S1·AMPPNP or S1·ADP·BeF_x may be so alike and yet the actin cross-linking patterns (and binding properties) appear to be so different. Either crystal packing altered the structure of these S1·nucleotide analogues, or very modest changes in the structure of the myosin head are sufficient to regulate the strength of the interface by many orders of magnitude. Which one of these two explanations is correct still remains to be seen.

Our data suggest different degrees of rotational freedom for S1 bound to actin filament, depending on the intermediate of the ATPase cycle. With the actin−S1·ATP intermediate, S1 is cross-linked to,-and may interact predominantly with, one actin monomer, and consequently, it should have a large degree of possible attachment angle. With the actin−S1·ADP·P_i intermediate, however, S1 binds to two actin monomers so that its rotational freedom is restricted, albeit not as much in the rigor complex due to the metastable character of the weak-binding interface. To relate these three classes of actin−S1 complexes to the disorder to order transition model proposed by EPR experiments (*50*), there must exist two subpopulations in the disordered state (actin−S1·ATP and actin−S1·ADP·P_i complexes) characterized by slightly different rotational freedoms.

Finally, electron microscopic analysis of the structure of the actin−S1 complex during ATP hydrolysis has been controversial. Early studies proposed two extreme attachment angles for S1 on actin filament (*84*), but more detailed analysis revealed two additional sets of images. In one case, S1 could adopt a wide variety of angles during the ATPase reaction (*45*, *66*, *85*), while in the other case, no difference in S1 orientation could be established between rigor and active complexes (*86*, *87*). Our data could eventually explain EM discrepancies if one considers that slight differences in experimental conditions (presence of methanol, different temperatures, etc.) might have shifted the limiting step of the ATPase reaction, leading to the formation of two different ternary complexes: the actin−S1·ATP intermediate with a high degree of disorder and the actin−S1·ADP·P_i intermediate with a final averaged orientation close to the rigor binding state.

Relation to Kinetic Data. It is not clear which of these three states of the actin−S1 interface is directly related to the three-step docking model proposed by Geeves and Conibear (*4*) on the basis of kinetic data. The simplest hypothesis would be that S1·ATP, S1·ADP·P_i, and S1 or S1·ADP populate preferentially the collision, the A-state, and the R-state complexes, respectively. But this hypothesis is not yet totally convincing since the interface in the actin−S1·ADP·P_i intermediate is mostly of ionic nature (*6*) and the hydrophobic components present (*37*) cannot account for the strongly hydrophobic nature of the interface in the A-state (*4*). In addition, this preworking stroke (A-state) is thought to be obtained only after γP_i release, generating the S1·ADP′ state which was recently proposed to contain a rather strong actin−S1 interface (*70*). To correlate unambiguously structural and kinetic data, one needs to characterize further the actin−S1·ADP′ complex which can apparently be stabilized with myosin from nonskeletal muscle tissues (*70*).

In conclusion, this work shows that the skeletal myosin head interacts with the N-terminal segment of two actin monomers, predominantly in the weak-binding state, i.e., during the formation of the actin−S1·ADP·P_i intermediate. Whether this behavior is specific for the skeletal actin−myosin complex, thus leading to a more efficient mechanochemical cycle, or whether it is widespread in all muscle and nonmuscle myosin remains to be discovered. The lack of strong sequence homology in the two corresponding S1 loops does not prevent the acceptance of this concept for two reasons. First, the actin binding subsites along the myosin sequences are not usually so well conserved (*88*), and second, S1 binding to two actin molecules may involve different subsites depending on the type of myosin. Further characterization of the interface of the actin−myosin complex of different sources will undoubtedly be needed to generalize the conclusions of this work.

ACKNOWLEDGMENT

We are very grateful to Dr. T. Barman and F. Travers for their helpful discussions and to T. Barman for the critical reading of the manuscript. Dr. N. Bonafé was associated with the very preliminary experiments performed in the presence of NHS and ATP.

REFERENCES

1. Lymn, R., and Taylor, E. D. (1971) *Biochemistry 10*, 4617−4624.
2. Bagshaw, C. R., and Trentham, D. R. (1974) *Biochem. J. 141*, 331−349.
3. Eisenberg, R., and Hill, T. L. (1985) *Science 277*, 999−1006.
4. Geeves, M. A., and Conibear, P. B. (1995) *Biophys. J. 68*, 194s−199s.
5. Ostap, E. M., and Pollard, T. D. (1996) *J. Cell Biol. 132*, 1053−1060.
6. Highsmith, S., and Murphy, A. J. (1992) *Biochemistry 31*, 385−389.
7. Janin, J. (1997) *Proteins 28*, 153−161.
8. Hibberg, M. G., and Trentham, D. R. (1986) *Annu. Rev. Biophys. Chem. 15*, 119−161.
9. Homsher, E., Lacktis, J., and Regnier, M. (1997) *Biophys. J. 72*, 1780−1791.
10. Highsmith, S. (1990) *Biochemistry 29*, 10690−10691.
11. Chaussepied, P., Morales, M. F., and Kassab, R. (1988) *Biochemistry 27*, 1778−1785.
12. Cooke, R. (1997) *Physiol. Rev. 77*, 671−697.
13. Rayment, I., Holden, H. M., Whittaker, M., Yohn, C. B., Lorenz, M., Holmes, K. C., and Milligan, R. A. (1993) *Science 261*, 58−65.
14. Schroder, R. R., Manstein, D. J., Jahn, W., Holden, H., Rayment, I., Holmes, K. C., and Spudich, J. A. (1993) *Nature 364*, 171−174.
15. Mendelson, R., and Morris, E. P. (1997) *Proc. Natl. Acad. Sci. U.S.A. 94*, 8533−8538.
16. Yamamoto, K. (1989) *Biochemistry 28*, 5573−5577.
17. Bertrand, R., Chaussepied, P., Audemard, E., and Kassab, R. (1989) *Eur. J. Biochem. 181*, 747−754.
18. Chaussepied, P., and Morales, M. F. (1988) *Proc. Natl. Acad. Sci. U.S.A. 85*, 7471−7475.
19. Chaussepied, P. (1989) *Biochemistry 28*, 9123−9128.
20. Cheung, P., and Reisler, E. (1992) *Biochem. Biophys. Res. Commun. 189*, 1143−1149.
21. Bobkov, A. A., Bobkova, E. A., Lin, S.-H., and Reisler, E. (1996) *Proc. Natl. Acad. Sci. U.S.A. 93*, 2285−2289.
22. DasGupta, G., and Reisler, E. (1991) *Biochemistry 30*, 9961−9976.

23. DasGupta, G., and Reisler, E. (1992) *Biochemistry 31*, 1836−1841.
24. Adams, S., and Reisler, E. (1993) *Biochemistry 32*, 5051−5056.
25. Miller, L., Kalnoski, M., Yunossi, Z., Bulinski, J. C., and Reisler, E. (1987) *Biochemistry 26*, 6064−6070.
26. Brenner, B., Kraft, T., DasGupta, G., and Reisler, E. (1996) *Biophys. J. 70*, 48−56.
27. Sutoh, K., Ando, M., Sutoh, K., and Toyoshima, Y. Y. (1991) *Proc. Natl. Acad. Sci. U.S.A. 88*, 7711−7714.
28. Johara, M., Toyoshima, Y. Y., Ishijima, A., Kojima, H., Yanagida, T., and Sutoh, K. (1993) *Proc. Natl. Acad. Sci. U.S.A. 90*, 2127−2131.
29. Kimberley Cook, R., Root, D., Miller, C., Reisler, E., and Rubenstein, P. A. (1993) *J. Biol. Chem. 268*, 2410−2415.
30. Miller, C. J., and Reisler, E. (1995) *Biochemistry 34*, 2694−2700.
31. Uyeda, T. Q., Ruppel, K. M., and Spudich, J. A. (1994) *Nature 368*, 567−569.
32. Rovner, A. S., Freyzon, Y., and Trybus, K. M. (1995) *J. Biol. Chem. 270*, 30260−30263.
33. Miller, C. J., Wong, W. W., Bobkova, E., Rubenstein, P. A., and Reisler, E. (1996) *Biochemistry 35*, 16557−16565.
34. Onishi, H., Morales, M. F., Katoh, K., and Fujiwara, K. (1995) *Proc. Natl. Acad. Sci. U.S.A. 92*, 11965−11969.
35. Patterson, B., and Spudich, J. A. (1996) *Genetics 143*, 801−810.
36. Giese, K. C., and Spudich, J. A. (1997) *Biochemistry 36*, 8465−8473.
37. Bertrand, R., Derancourt, J., and Kassab, R. (1997) *Biochemistry 36*, 9703−9714.
38. Andreev, O. A., and Borejdo, J. (1992) *J. Muscle Res. Cell Motil. 13*, 523−533.
39. Bonafé, N., and Chaussepied, P. (1995) *Biophys. J. 68*, 35s−43s.
40. Xiao, M., Andreev, O. A., and Borejdo, J. (1995) *J. Mol. Biol. 248*, 294−307.
41. Mornet, D., Bertrand, R., Pantel, P., Audemard, E., and Kassab, R. (1981) *Nature 292*, 301−306.
42. Sutoh, K. (1982) *Biochemistry 21*, 3654−3661.
43. Sutoh, K. (1983) *Biochemistry 22*, 1579−1585.
44. Chen, T., Applegate, D., and Reisler, E. (1985) *Biochemistry 24*, 5620−5625.
45. Craig, R., Greene, L. E., and Eisenberg, E. (1985) *Proc. Natl. Acad. Sci. U.S.A. 82*, 3247−3251.
46. Arata, T. (1986) *J. Mol. Biol. 191*, 107−116.
47. Elzinga, M. (1987) in *Methods in Protein Science Analysis* (Walsh, K. E., Ed.) pp 615−623, Humana Press, Totowa, NJ.
48. Grabarek, Z., and Gergely, J. (1990) *Anal. Biochem. 185*, 131−135.
49. Gulick, A. M., Bauer, C. B., Thoden, J. B., and Rayment, I. (1997) *Biochemistry 36*, 11619−11628.
50. Roopnarin, O., and Thomas, D. D. (1996) *Biophys. J. 70*, 2795−2806.
51. Duong, A. M., and Reisler, E. (1989) *Biochemistry 28*, 3502−3509.
52. Fisher, A. J., Smith, C. A., Thoden, J. B., Sutoh, K., Holden, H. M., and Rayment, I. (1995) *Biochemistry 34*, 8960−8972.
53. Smith, C. A., and Rayment, I. (1996) *Biochemistry 35*, 5404−5417.
54. Burke, M., Reisler, E., and Harrington, W. F. (1976) *Biochemistry 15*, 1923−1927.
55. Offer, G., Baker, H., and Baker, L. (1972) *J. Mol. Biol. 66*, 435−444.
56. Weeds, A. G., and Taylor, R. A. (1975) *Nature 257*, 54−56.
57. Lheureux, K., Forne, T., and Chaussepied, P. (1993) *Biochemistry 32*, 10005−10014.
58. Eisenberg, E., and Kielley, W. W. (1974) *J. Biol. Chem. 249*, 4742−4748.
59. Wells, J. A., and Yount, R. G. (1980) *Biochemistry 19*, 1711−1717.
60. Chalovich, J. M., Greene, L. E., and Eisenberg, E. (1983) *Proc. Natl. Acad. Sci. U.S.A. 80*, 4909−4913.
61. Goodno, C. C. (1982) *Methods Enzymol. 85*, 116−123.
62. Bradford, M. M. (1976) *Anal. Biochem. 72*, 248−254.
63. Laemmli, U. K. (1970) *Nature 227*, 680−685.
64. Andreev, O. A., and Borejdo, J. (1995) *Biochemistry 34*, 14829−14833.
65. Combeau, C., Didry, D., and Carlier, M. F. (1992) *J. Biol. Chem. 267*, 14038−14046.
66. Walker, M., White, H., Belknap, B., and Trinick, J. (1994) *Biophys. J. 66*, 1563−1572.
67. Bagshaw, C. R., Eccleston, J. F., Trentham, D. R., Yates, D. W., and Goody, R. S. (1972) *Cold Spring Harbor Symp. Quant. Biol. 37*, 127−135.
68. Resetar, A. M., and Chalovich, J. M. (1995) *Biochemistry 34*, 16039−16045.
69. Andreeva, A. L., Andreev, O. A., and Borejdo, J. (1993) *Biochemistry 32*, 13956−13960.
70. Jontes, J. D., and Milligan, R. A. (1997) *J. Cell Biol. 139*, 683−693.
71. Rosenfeld, S. S., and Taylor, E. W. (1984) *J. Biol. Chem. 259*, 11908−11919.
72. Tesi, C., Barman, T., and Travers, F. (1991) *FEBS Lett. 260*, 229−232.
73. White, H. D., Belknap, B., and Webb, M. R. (1997) *Biochemistry 36*, 11828−11836.
74. Cherfils, J., Ménétrey, J., LeBras, G., LeBras, G., Janoeix-Lerosey, I., Gunsburg, J., Garel, J.-R., and Auzat, I. (1997) *EMBO J. 16*, 5582−5591.
75. Bertrand, R., Chaussepied, P., Kassab, R., Boyer, M., Roustan, C., and Benyamin, Y. (1988) *Biochemistry 27*, 5728−5736.
76. Von Hippel, P. H., and Berg, O. G. (1989) *J. Biol. Chem. 264*, 675−678.
77. Blotnik, E., Miller, C., Groschel-Stewart, U., and Muhlrad, A. (1995) *Eur. J. Biochem. 232*, 235−240.
78. Werber, M. M., Peyser, Y. M., and Muhlrad, A. (1992) *Biochemistry 31*, 7190−7197.
79. Bobkov, A. A., Sutoh, K., and Reisler, E. (1997) *J. Muscle Res. Cell Motil. 18*, 563−571.
80. Combeau, C., and Carlier, M. F. (1988) *J. Biol. Chem. 263*, 17429−17436.
81. Muhlrad, A., Cheung, P., Phan, B. C., Miller, C., and Reisler, E. (1994) *J. Biol. Chem. 269*, 11852−11858.
82. Kirshenbaum, K., Papp, S., and Highsmith, S. (1995) *Biophys. J. 65*, 1121−1129.
83. Diaz Banos, F. G., Bordas, J., Lowy, J., and Svensson, A. (1996) *Biophys. J. 71*, 576−589.
84. Huxley, H. E. (1969) *Science 164*, 1356−1366.
85. Applegate, D., and Flicker, F. (1987) *J. Biol. Chem. 262*, 6856−6863.
86. Funatsu, T., Kono, E., and Tsukita, S. (1993) *J. Cell Biol. 121*, 1053−1064.
87. Pollard, T. D., Bhandari, D., Maupin, P., Wachsstock, D., Weeds, A. G., and Zot, H. G. (1993) *Biophys. J. 64*, 454−471.
88. Coope, T. V., Whisstock, J., Rayment, I., and Kendrick-Jones, J. (1996) *Structure 4*, 969−987.

BI980139A